

Modeling Formation of Globular Clusters: Beacons of Galactic Star Formation

Oleg Y. Gnedin

University of Michigan, Department of Astronomy, Ann Arbor, MI 48109, USA
 ognedin@umich.edu

Abstract. Modern hydrodynamic simulations of galaxy formation are able to predict accurately the rates and locations of the assembly of giant molecular clouds in early galaxies. These clouds could host star clusters with the masses and sizes of real globular clusters. I describe current state-of-the-art simulations aimed at understanding the origin of the cluster mass function and metallicity distribution. Metallicity bimodality of globular cluster systems appears to be a natural outcome of hierarchical formation and gradually declining fraction of cold gas in galaxies. Globular cluster formation was most prominent at redshifts $z > 3$, when massive star clusters may have contributed as much as 20% of all galactic star formation.

Keywords. galaxies: formation — galaxies: star clusters — globular clusters: general

1. Clues from Old and Young Star Clusters

A self-consistent description of the formation of globular clusters remains a challenge to theorists. Most of the progress is driven by observational discoveries. The Hubble Space Telescope observations have convincingly demonstrated one of the likely routes for the formation of massive star clusters today – in the mergers of gas-rich galaxies. These observations have also shown the differences between the mass function of young clusters (power-law $dN/dM \propto M^{-2}$) and old clusters (log-normal or broken power-law).

Surveys of the globular cluster systems of galaxies in the Virgo and Fornax galaxy clusters have solidified the evidence for bimodal, and even multimodal, color distribution in galaxies ranging from dwarf disks to giant ellipticals (Peng et al. 2008). This color bimodality likely translates into a bimodal distribution of the abundances of heavy elements such as iron. We know this to be the case in the Galaxy as well as in M31, where accurate spectral measurements exist for a large fraction of the clusters. The two most frequently encountered modes are commonly called *blue* (metal-poor) and *red* (metal-rich).

Detailed spectroscopy reveals a significant spread of ages of the red clusters in the Galaxy, up to 6 Gyr (Dotter et al. 2010). The spread increases with metallicity and distance from the center. The age spread of the blue clusters is smaller, in the range 1-2 Gyr, and is consistent with the measurement errors.

2. Modeling the Formation of Globular Clusters is Hard

The first attempt to model the formation of globular clusters within the framework of hierarchical galaxy formation was by Beasley et al. (2002). Their semi-analytical model could reproduce the metallicity bimodality only by assuming two separate prescriptions for the blue and red clusters: blue clusters formed in quiescent disks with an efficiency of 0.002 relative to field stars, whereas red clusters formed in gas-rich mergers with a higher efficiency of 0.007. The formation of blue clusters also had to be artificially halted after $z = 5$, so as not to dilute the bimodality.

Moore et al. (2006) considered an idealized scenario for the formation of blue globular clusters at high redshift, inside dark matter halos that would eventually merge into the Galaxy, one cluster per halo. They used the observed spatial distribution of the Galactic clusters to constrain the formation epoch and found that the clusters would need to form by $z \sim 12$, in relatively small halos. Such an early formation is inconsistent with the simultaneous requirements of high mass and density for the parent molecular clouds to produce such dense ($\rho_* > 10^4 \text{ M}_\odot \text{ pc}^{-3}$) and massive ($M > 10^5 \text{ M}_\odot$) clusters as observed. This scenario also places stringent constraints on the age spread of blue clusters to be less than 0.5 Gyr, which may already be inconsistent with the available age measurements. The tension with observations of this scenario, and of its several variants in the literature, probably indicates that globular clusters cannot be simply associated with early dark matter halos and, instead, must be studied as an integral part of galactic star formation.

3. Globular Clusters Could Form in Protogalactic Disks

Kravtsov & Gnedin (2005) used a hydrodynamic simulation of a Galactic environment at redshifts $z > 3$ and found dense, massive gas clouds within the protogalactic clumps. These clouds assemble within the self-gravitating disk of progenitor galaxies after gas-rich mergers. The disk develops strong spiral arms, which further fragment into separate molecular clouds located along the arms as beads on a string. A working assumption, that the central high-density region of these clouds formed a star cluster, results in the distributions of cluster mass, size, and metallicity that are consistent with those of the Galactic metal-poor clusters. The high stellar density of Galactic clusters restricts their parent clouds to be in relatively massive progenitors, with the total mass $M_h > 10^9 \text{ M}_\odot$. The mass of the molecular clouds increases with cosmic time, but the rate of mergers declines steadily. Therefore, the cluster formation efficiency peaks during an extended epoch, $5 < z < 3$, when the Universe is still less than 2 Gyr old. The parent molecular clouds are massive enough to be self-shielded from UV radiation, so that globular cluster formation should be unaffected by the reionization of cosmic hydrogen at $z > 6$. The mass function of model clusters is consistent with a power law $dN/dM \propto M^{-2}$, similar to the local young star clusters. The total mass of clusters formed in each progenitor is roughly proportional to the available gas supply and the total mass, $M_{GC} \sim 10^{-4} M_h$.

Prieto & Gnedin (2008) showed that subsequent mergers of the progenitor galaxies would ensure the present distribution of the globular cluster system is spheroidal, as observed, even though initially all clusters form on nearly circular orbits. Depending on the subsequent trajectories of their host galaxies, clusters form three main subsystems at present time. *Disk clusters* formed in the most massive progenitor that eventually hosts the present Galactic disk. These clusters are scattered into eccentric orbits by perturbations from accreted galactic satellites. *Inner halo clusters* came from the now-disrupted satellite galaxies. Their orbits are inclined with respect to the Galactic disk and are fairly isotropic. *Outer halo clusters* are either still associated with the surviving satellite galaxies, or were scattered away from their hosts during close encounters with other satellites and consequently appear isolated.

Following the scenario outlined above, Muratov & Gnedin (2010) developed a semi-analytical model that aims to reproduce statistically the metallicity distribution of the Galactic globular clusters. The formation of clusters is triggered during a merger of gas-rich protogalaxies with the mass ratio 1:5 or higher, and during very early mergers with any mass ratio when the cold gas fraction in the progenitors is close to 100%. Model clusters are assigned the mean metallicity of their host galaxies, which is calculated using the observed galaxy stellar mass-metallicity relation.

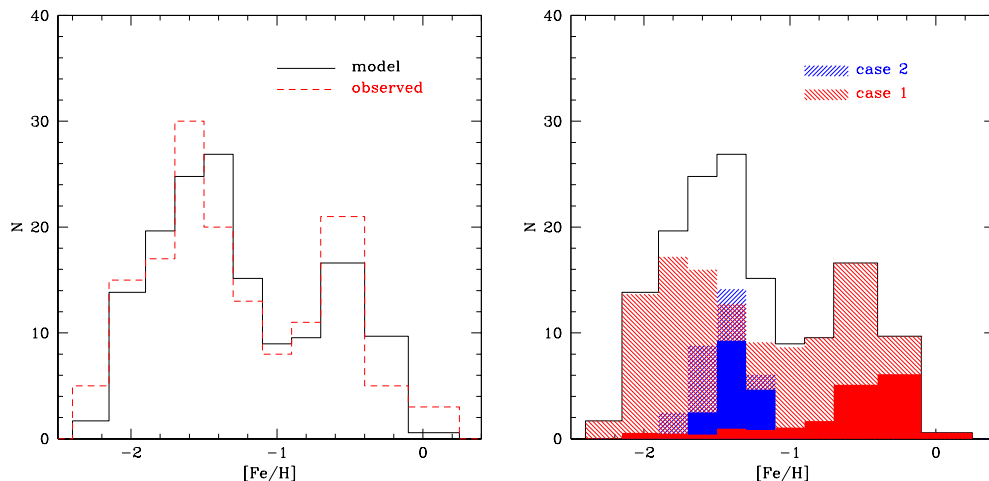


Figure 1. *Left:* Metallicities of model clusters that survived dynamical disruption until $z = 0$, compared to the observed distribution of Galactic globular clusters. *Right:* Model metallicity distribution split by the formation criterion: major mergers (**case-1**) and early mergers (**case-2**). Filled histograms show clusters formed in the main Galactic disk. From Muratov & Gnedin (2010).

4. Metallicity Bimodality

Figure 1 shows the metallicity bimodality in the model of Muratov & Gnedin (2010). Note that the model imposes the same formation criteria for all clusters, without explicitly differentiating between the two modes. The only variables are the gradually changing amount of cold gas, the growth of protogalactic disks, and the rate of merging. Yet, the model produces two peaks of the metallicity distribution, centered at $[\text{Fe}/\text{H}] \approx -1.6$ and $[\text{Fe}/\text{H}] \approx -0.6$, matching the Galactic globular clusters.

The red peak is not as pronounced as in the observations but is still significant. Early mergers of low-mass progenitors contribute only blue clusters. Interestingly, later major mergers contribute both to the red and blue modes, in about equal proportions. They are expected to produce a higher fraction of red clusters in galaxies with more active merger history, such as in massive ellipticals.

In this scenario, bimodality results from the history of galaxy assembly (rate of mergers) and the amount of cold gas in protogalactic disks. Early mergers are frequent but involve relatively low-mass protogalaxies, which produce preferentially blue clusters. Late mergers are infrequent but typically involve more massive galaxies. As the number of clusters formed in each merger increases with the progenitor mass, just a few late super-massive mergers can produce a significant number of red clusters. The concurrent growth of the average metallicity of galaxies between the late mergers leads to an apparent “gap” between the red and blue clusters.

Our prescription links cluster metallicity to the average galaxy metallicity in a one-to-one relation, albeit with random scatter. Since the average galaxy metallicity grows monotonically with time, the cluster metallicity also grows with time. The model thus encodes an age-metallicity relation, in the sense that metal-rich clusters are younger than their metal-poor counterparts by several Gyr. However, clusters of the same age may differ in metallicity by as much as a factor of 10, as they formed in the progenitors of different mass.

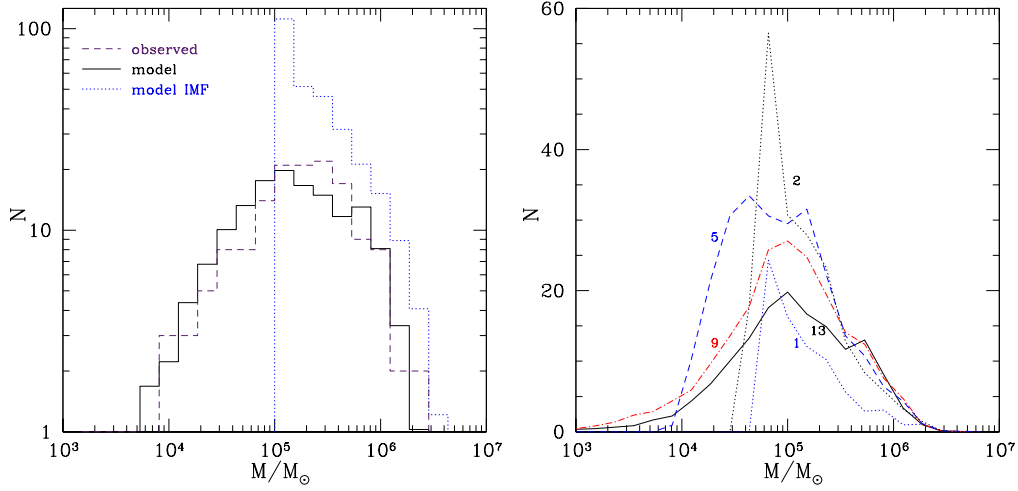


Figure 2. *Left:* Dynamically evolved model clusters at $z = 0$ (solid), compared to the Galactic globular clusters (dashed). Dotted histogram shows the combined initial masses of model clusters with $M > 10^5 M_\odot$ formed at all epochs, including those that did not survive until the present. *Right:* Evolution of the mass function at cosmic times of 1 Gyr ($z \approx 5.7$, dotted), 2 Gyr ($z \approx 3.2$, dotted), 5 Gyr ($z \approx 1.3$, dashed), 9 Gyr ($z \approx 0.5$, dot-dashed), and 13.5 Gyr ($z = 0$, solid).

5. Evolution of the Mass Function

Some of the old and low-mass clusters will be disrupted by the gradual escape of stars and will not appear in the observed sample. Figure 2 shows the dynamical evolution of the cluster mass function, as a result of stellar mass loss, tidal truncation, and two-body evaporation. Even though the model parameters were tuned to reproduce the metallicity, not the mass distribution, the mass function at $z = 0$ is consistent with the observed in the Galaxy. Majority of the disrupted clusters were blue clusters that formed in early low-mass progenitors.

Right panel of Figure 2 illustrates the interplay between the continuous buildup of massive clusters ($M > 10^5 M_\odot$) and the dynamical erosion of the low-mass clusters ($M < 10^5 M_\odot$). Expecting that most clusters below $10^5 M_\odot$ would eventually be disrupted, we did not track their formation in the model. Instead, the low end of the mass function is built by the gradual evaporation of more massive clusters. Note that most of the clusters were not formed until the universe was 2 Gyr old, corresponding to $z \approx 3$. The fraction of clusters formed before $z \approx 6$, when cosmic hydrogen was reionized, is small.

An exciting prediction of the model is a high fraction of galaxy stellar mass locked in star clusters at $z > 3$: $M_{GC}/M_* \approx 10 - 20\%$. This fraction declines steadily with time and reaches 0.1% at the present epoch.

References

- Beasley, M. A., Baugh, C. M., Forbes, D. A. et al. 2002, *MNRAS*, 333, 383
- Dotter, A., Sarajedini, A., Anderson, J. et al. 2010, *ApJ*, 708, 698
- Kravtsov, A. V. & Gnedin, O. Y. 2005, *ApJ*, 623, 650
- Moore, B., Diemand, J., Madau, P., Zemp, M., & Stadel, J. 2006, *MNRAS*, 368, 563
- Muratov, A. L. & Gnedin, O. Y. 2010, *ApJ*, 718, 1266
- Peng, E. W., Jordán, A., Côté, P. et al. 2008, *ApJ*, 681, 197
- Prieto, J. L. & Gnedin, O. Y. 2008, *ApJ*, 689, 919